Journal of Hazardous Materials 179 (2010) 295–302

Contents lists available at ScienceDirect

Journal of Hazardous Materials

journal homepage: www.elsevier.com/locate/jhazmat

Adsorptive recovery of UO_2^{2+} from aqueous solutions using collagen–tannin resin

Xia Sun [a], Xin Huang [a], Xue-pin Liao [a,b,*], Bi Shi [b]

[a] Department of Biomass Chemistry and Engineering, Sichuan University, Chengdu 610065, China
[b] National Engineering Laboratory for Clean Technology of Leather Manufacture, Sichuan University, Chengdu 610065, China

ARTICLE INFO

Article history:
Received 4 November 2009
Received in revised form 3 February 2010
Accepted 2 March 2010
Available online 7 March 2010

Keywords:
Collagen–tannin resin
Uranium (UO_2^{2+})
Adsorption
Column adsorption

ABSTRACT

Collagen–tannin resin (CTR), as a novel adsorbent, was prepared via reaction of collagen with black wattle tannin and aldehyde, and its adsorption properties to UO_2^{2+} were investigated in detail, including pH effect, adsorption kinetics, adsorption equilibrium and column adsorption kinetics. The adsorption of UO_2^{2+} on CTR was pH-dependent, and the optimal pH range was 5.0–6.0. CTR exhibited excellent adsorption capacity to UO_2^{2+}. For instance, the adsorption capacity obtained at 303 K and pH 6.0 was as high as 0.91 mmol UO_2^{2+}/g when the initial concentration of UO_2^{2+} was 1.0 mmol/L. In kinetics studies, the adsorption equilibrium can be reached within 300 min, and the experimental data were well fitted by the pseudo-second-order rate model, and the equilibrium adsorption capacities calculated by the model were almost the same as those determined by experiments. The adsorption isotherms could be well described by the Freundlich equation with the correlation coefficients (R^2) higher than 0.99, the adsorption behaviors of UO_2^{2+} on CTR column were investigated as well. Present study suggested that the CTR can be used for the adsorptive recovery of UO_2^{2+} from aqueous solutions.

1. Introduction

Uranium is one of the most important elements for nuclear industry, which has significant commercial use as a fuel for electricity generation. Due to its strong radiation, uranium is extremely harmful to human beings, and uranium contamination can also cause serious environmental problems. In general, the uranium released into environment is often dissolved in aqueous solutions, which is predominant in hexavalent form as UO_2^{2+}. Therefore, the recovery of uranium from aqueous solutions is essential important in view of nuclear fuel resource and human health.

The general methods developed for the recovery or removal of hexavalent uranium ions from aqueous solutions are extraction [1], precipitation [2,3], ion exchange [4] and adsorption [5]. Among those approaches, adsorption is commonly used for the recovery of uranium ions at relatively low concentration. It is reported that some minerals [6], phosphates [7], poly-resins [8] and microorganisms [9] have been used as adsorbents for the recovery of UO_2^{2+} from wastewater. However, the adsorption capacity and selectivity of those adsorbents to UO_2^{2+} need to be improved.

It has been reported that plant tannins exhibit specific affinity towards many metal ions [10], due to their abundant of multiple adjacent hydroxyl groups (as shown in Fig. 1). Thus, tannins can be probably used for the purpose of UO_2^{2+} recovery from aqueous solutions. However, tannins are water-soluble and cannot directly be used for the adsorptive recovery of UO_2^{2+} from wastewater. To overcome this disadvantage, many attempts had been made to immobilize tannins onto various water-insoluble matrices. It has been reported that tannins can be immobilized onto agarose [11], viscose rayon fiber [12], cellulose [13] and other matrices [14]. Our previous investigations indicated that tannins can be immobilized onto collagen fiber through a cross-linking reaction with aldehydes [15], and these immobilized tannins exhibited excellent adsorption capacities to many metal ions [16,17]. For the adsorption of UO_2^{2+}, collagen fiber immobilized tannins (CF-T) has an adsorption capacity of 0.65 mmol/g under the optimized conditions [16]. However, the adsorption capacity of CF-T to UO_2^{2+} still has room for improvement due to the fact that collagen fiber is tightly braided, which results in a limited loading amount of tannins. In fact, the amount of tannins immobilized onto CF-T was lower than 0.5 g/g [16,17]. Therefore, it is reasonable to hypothesize that an adsorbent with higher adsorption capacity to UO_2^{2+} could be prepared if we can find a method to increase the amount of tannins immobilized onto collagen matrix.

In this study, collagen fiber was hydrolyzed into collagen and then reacted with black wattle tannin to prepare collagen–tannin

* Corresponding author at: Department of Biomass Chemistry and Engineering, Sichuan University, Chengdu 610065, China. Tel.: +86 28 85400382; fax: +86 28 85460356.
E-mail address: xpliao@scu.edu.cn (X.-p. Liao).

0304-3894/$ – see front matter © 2010 Elsevier B.V. All rights reserved.
doi:10.1016/j.jhazmat.2010.03.002

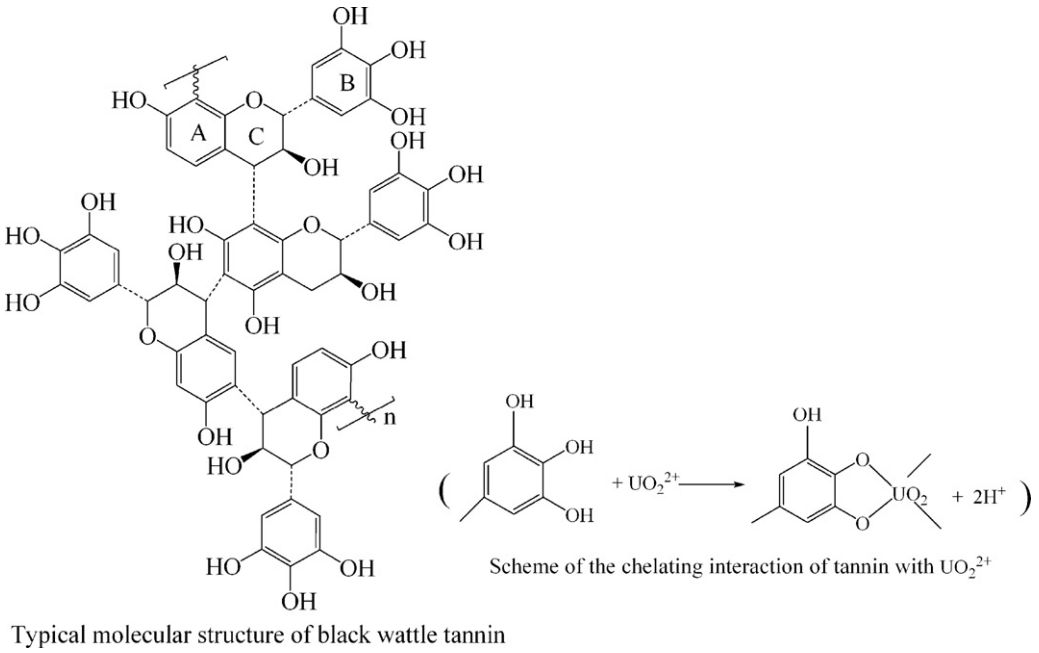

Fig. 1. Schemes of molecular structure of black wattle tannin and its chelating interaction with UO_2^{2+}.

resin (CTR). It can be inferred that the amount of tannins immobilized onto collagen should be significantly increased because the functional groups of hydrolyzed collagen are fully exposed outside during the reaction process, and therefore, a higher adsorption capacity to UO_2^{2+} can be expected. Consequently, the objective of this article was to investigate the adsorption behaviors of UO_2^{2+} on CTR, including pH effect, adsorption kinetics, adsorption isotherms and column adsorption.

2. Materials and methods

2.1. Reagents

The UO_2^{2+} stock solution (10.0 mmol/L) was prepared by dissolving uranyl nitrate [$UO_2(NO_3)_2{\cdot}6H_2O$] in deionized water. Black wattle tannin was extracted from the barks of black wattle, and the tannin content of the extract was about 78% (wt%). All of the other chemicals used in the study were of analytical grade. The pH adjustment of solutions was carried out using 0.5 mol/L HNO_3 and/or 0.5 mol/L NaOH solutions.

2.2. Preparation of CTR

According to the approaches of leather manufacturing [18], the calf pelt was cleaned, unhaired, limed, splitted and delimed in order to remove the non-collagen components. Then the pelt was cut into smaller pieces and further pulverized in a mill. 40.0 g of milled calf skin (water content was 80%) was suspended in 800.0 mL of 0.5 mol/L acetic acid solution. Then, 1.3 g of pepsin (activity, 12,000 U/g) was added, and the hydrolyzation of collagen fiber was conducted at 277–283 K for 24 h. The obtained hydrolyzate was first centrifuged and then salted-out using 2.0 mol/L NaCl, and the calf skin collagen in gel state was obtained.

24.0 g of black wattle tannin dissolved in 80.0 mL of deionized water was mixed with collagen prepared above. The mixture was stirred at 298 K for 3 h, and then continuously stirred at 313 K for 1 h. After the intermediate product was collected by filtration, 200.0 mL of 5% (wt%) oxazolidine solution (cross-linking agent) at pH 6.5 was added. The mixture was kept stirring at 298 K for 2 h, and then continuously reacted at 313 K for another 2 h. Subsequently, the product was collected by filtration, thoroughly washed with deionized water and vacuum dried at 298 K for 12 h. Finally, collagen–tannin resin (CTR) was obtained.

2.3. Batch adsorption studies

2.3.1. Effect of initial pH on the adsorption capacity

100.0 mg of CTR was suspended in each 100.0 mL of 1.0 mmol/L UO_2^{2+} solutions where the initial pH is 2.0, 3.0, 4.0, 5.0, 6.0 and 7.0, respectively. Adsorption experiments were conducted by constant shaking at 303 K for 24 h. The concentration of UO_2^{2+} in residual solution after adsorption was analyzed by Inductively Coupled Plasma Atomic Emission Spectrometer (ICP-AES, PerkinElmer Optima 2100DV, USA). The adsorption capacities at different initial pH were obtained by mass balance calculation and were denoted as q_e (mmol/g). In order to ascertain the chelation extent of UO_2^{2+} by the –OH groups of black wattle tannin, we carried out the attenuated total reflectance-Fourier Transform Infrared (ATR-FTIR) spectral studies of collagen–tannin resin (CTR) before and after adsorption of UO_2^{2+}. The amount of CTR and CTR-UO_2^{2+} used in ATR-FTIR spectral studies is identical.

2.3.2. Adsorption kinetics

100.0 mg of CTR was suspended in each 100.0 mL of 1.0 mmol/L UO_2^{2+} solutions. The pH of the solution was adjusted to 5.0. Adsorption was conducted by constant stirring at 303, 313 and 323 K, respectively. The concentration of UO_2^{2+} in residual solutions was analyzed at a regular interval by ICP-AES during adsorption process. The adsorption capacities at time t (min) were obtained by mass balance calculation and were denoted as q_t (mmol/g).

2.3.3. Adsorption isotherms

Isotherm studies were carried out with initial concentration of UO_2^{2+} ranging from 0.5 to 2.5 mmol/L. The pH of the solutions was adjusted to 5.0, and the adsorption experiments were conducted with constant stirring for 24 h at 303, 313 and 323 K, respectively. The concentration of UO_2^{2+} in residual solution after adsorption was analyzed by ICP-AES.

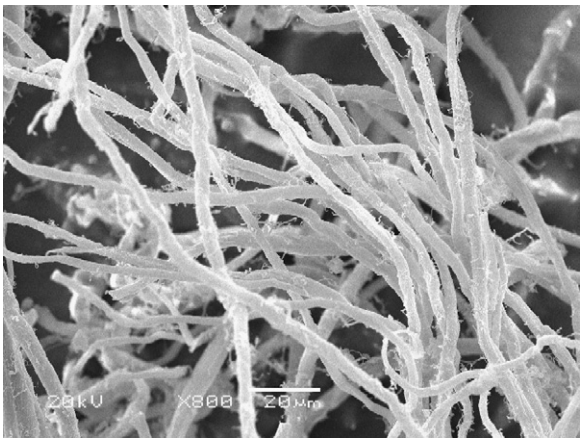

Fig. 2. SEM image of CTR.

All experiments were replicated three times and the errors were found to be within 5%.

2.4. Column adsorption

Column adsorption was performed on a perspex column (inner diameter = 1.1 cm) packed with CTR. A flow controller was used to control the inlet flow rate. The effluent was collected by an automatic collector, and then analyzed using ICP-AES. The effects of bed height and co-existing metal ions on column adsorption behavior were investigated. In addition, the reusability of the CTR column was also investigated.

3. Results and discussion

3.1. Characterization of CTR

It has been reported that calf skin collagen predominantly consists of rod-like type I collagen, of which the molecule is 1.5 nm in diameter and 300.0 nm in length [19]. In addition, type I collagen molecule has a tendency to linear assembly [20], and its assembly tendency can be promoted by the addition of other reagents [21,22]. These facts suggested that calf skin collagens may be induced by black wattle tannin to assembled into fibers, and simultaneously, black wattle tannin can be immobilized onto those assembled collagen fibers. In general, the interaction of tannins with collagen matrix is mainly due to the formation of hydrogen bonds and hydrophobic bonds, which means that tannin maybe leaked out in water or organic solvents during adsorption process. To prevent the leakage of tannins from CTR, we use oxazolidine as the cross-linking agent (as described in Section 2.2) to covalently immobilize tannins onto collagen matrix [23]. Ultraviolet–visible spectroscopy (UV–vis) indicates that there is no tannin leaked out in the residual solution during adsorption experiments.

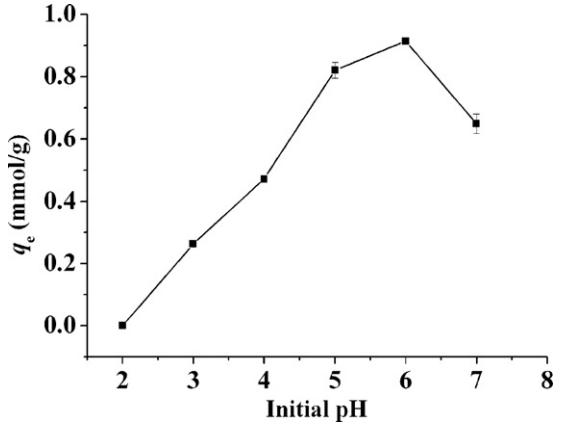

Fig. 3. Effect of initial pH on the adsorption capacity of UO_2^{2+} on CTR.

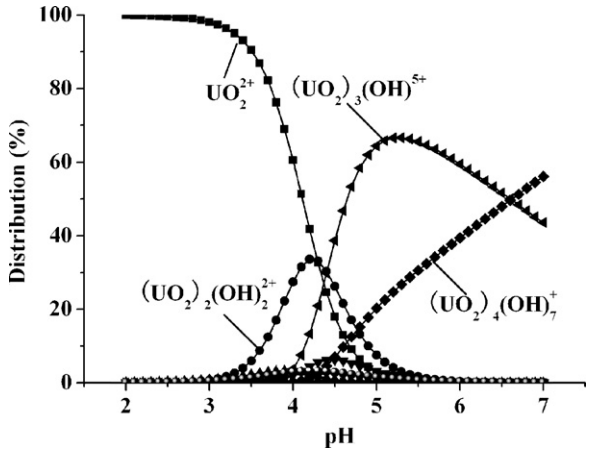

Fig. 4. Distribution of UO_2^{2+} species in aqueous solution at different pHs (calculated by Visual MINEQL 2.4b version, NIST database. Initial conc. of UO_2^{2+} = 1.0 mmol/L).

Surface morphology of CTR adsorbent is observed by scanning electronic microscope (SEM). As shown in Fig. 2, it is obvious that CTR is in fibrous state, implying that the collagen molecules indeed re-assembled together to form fibers by the inducement of black wattle tannin. Based on UV–vis analysis, the loading amount of tannins on CTR is determined to be 1.5 g/g, three times higher than that on CF-T (0.5 g/g), which indicates a much higher adsorption capacity to UO_2^{2+}. The pH corresponding to zero point of charge (pH_{zpc}) of the CTR is determined using solid addition method [24], and it is found that the pH_{zpc} of CTR is around 4.05 [as shown in supporting information (SI) 1].

3.2. Batch adsorption

3.2.1. Effect of initial pH on adsorption capacity

The effect of initial pH on the adsorption capacity of UO_2^{2+} on CTR is shown in Fig. 3. It is observed that the adsorption capacity is significantly influenced by pH. As pH increases from 2.0 to 6.0, the adsorption capacity increases gradually, and the maximum adsorption capacity achieves 0.91 mmol/g at pH 6.0, much higher than that of CF-T (0.65 mmol/g) [16]. This fact indicates that the increasing amount of tannin immobilized onto collagen matrix is accompanied by the increase of adsorption capacity to UO_2^{2+}. Thermodynamic analysis indicates that UO_2^{2+} mainly exists as UO_2^{2+}, $(UO_2)_2(OH)_2^{2+}$, $(UO_2)_3(OH)^{5+}$, $(UO_2)_4(OH)_7^{+}$ in the pH range of 2.0–7.0, as shown in Fig. 4. In the pH range of 2.0–4.05, the surface of CTR is positively charged because the solution pH is lower than the pH_{zpc} of CTR. Thus, the chelating interaction of UO_2^{2+} with phenolic hydroxyls of black wattle tannin is suppressed, and the adsorption capacity is relatively lower. When the solution pH is higher than the pH_{zpc} of CTR, the surface of CTR is negatively charged and more phenolic hydroxyls of black wattle tannin are ionized at higher pH, which significantly promotes the chelating interaction of UO_2^{2+} with CTR, resulting in an obvious increase of adsorption capacity in the range of 4.05–6.0. However, the phenolic hydroxyls of tannin can be easily oxidated to quinone at even higher pH (pH > 7.0), resulting in a loss of adsorption capacity to UO_2^{2+}. As a result, the suitable pH range for UO_2^{2+} adsorption should be 5.0–6.0. So the following experiments were all carried out at initial pH 5.0. Additionally, the solution pH was decreased after the adsorption process performed, which indicates that the hydrogen protons of phenolic

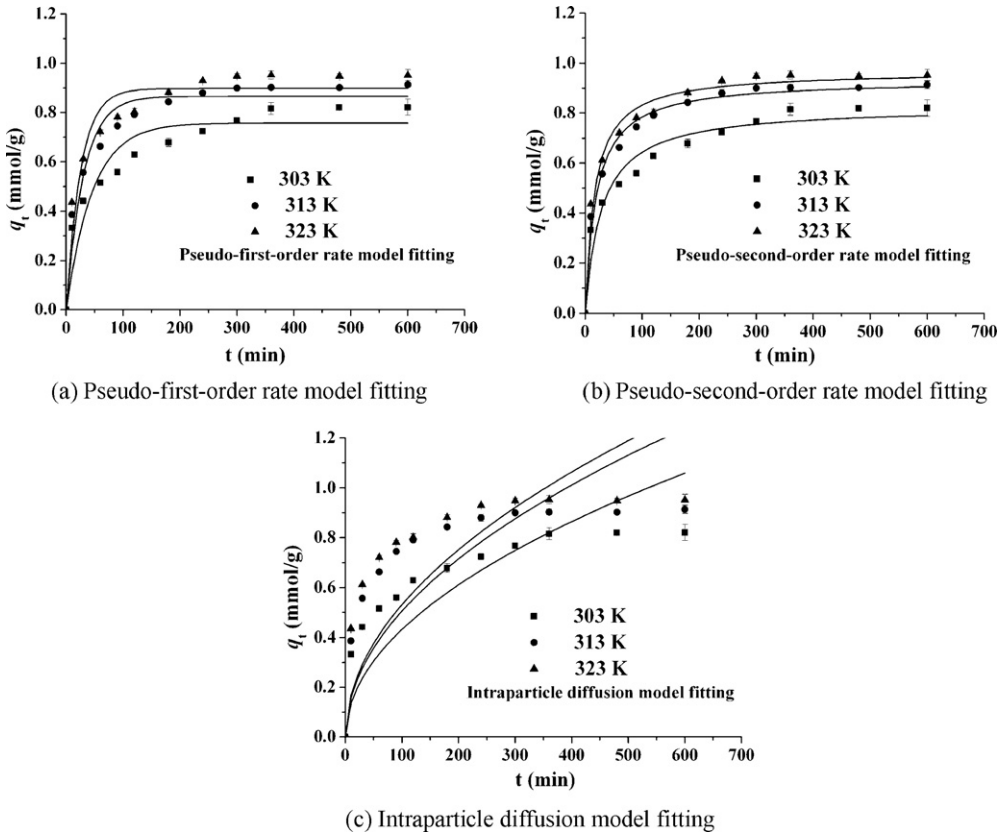

(a) Pseudo-first-order rate model fitting

(b) Pseudo-second-order rate model fitting

(c) Intraparticle diffusion model fitting

Fig. 5. Adsorption kinetics of CTR to UO_2^{2+}. (a) Pseudo-first-order rate model fitting; (b) pseudo-second-order rate model fitting; (c) intraparticle diffusion model fitting.

hydroxyls of tannin are released into solutions during adsorption process.

The remarkable influence of pH on the adsorption capacity suggests that the adsorption of CTR to UO_2^{2+} is dominated by surface complexation [25]. According to literature [15–17], many metal ions can chelate with the phenolic hydroxyls of the tannin to form a five-membered chelating ring. Accordingly, it is reasonable to infer that UO_2^{2+} should also be able to chelate with the phenolic hydroxyls of tannin. Subsequently, the attenuated total reflectance-Fourier transform infrared (ATR-FTIR) spectra of CTR before and after the adsorption of UO_2^{2+} are carried out (SI 2). The characteristic peak of UO_2^{2+} is clearly observed at 909.27 cm^{-1} [26], which confirms the adsorption of UO_2^{2+} on CTR. Additionally, the peak at 3304 cm^{-1}, which is associated to –OH groups of black wattle tannin, exhibits an obvious decrease of intensity, which confirms the chelating interaction of UO_2^{2+} with the –OH groups of black wattle tannin. Based on the integral calculation, about 26.44% of –OH groups of black wattle tannin are chelated with UO_2^{2+} when 0.1 g of CTR is used for the adsorption of 100.0 mL of UO_2^{2+} at pH 5.0.

3.2.2. Adsorption kinetics

The adsorption kinetics of UO_2^{2+} on CTR are shown in Fig. 5. It can be observed that the adsorption rate UO_2^{2+} on CTR is quite rapid, and the adsorption equilibrium attained is in about 300 min. Similar adsorption kinetics can be obtained under different temperatures. Compared with porous adsorbents, CTR is in fiber state and its specific area is limited (0.75–1.0 m^2/g) which suggested that the adsorption of UO_2^{2+} should take place at the outer surface of CTR, and that the intraparticle diffusion resistance could be neglected.

To confirm our prediction, the adsorption kinetic data are further analyzed using the pseudo-first-order rate model [27,28], the pseudo-second-order rate model [29] and the intraparticle diffusion model [30]:

$$\log(q_e - q_t) = \log q_e - \frac{k_1}{2.303}t \quad (1)$$

$$\frac{t}{q_t} = \frac{1}{k_2 q_e^2} + \frac{t}{q_e} \quad (2)$$

$$q_t = k_3 t^{0.5} \quad (3)$$

where q_e and q_t are the amounts of UO_2^{2+} adsorbed (mmol/g) at equilibrium and at time t (min), respectively, and k_1 (min^{-1}) and k_2 (g/(mmol min)) are the rate constant, k_3 (mmol/g $min^{-0.5}$) is the intraparticle diffusion rate constant.

The “pseudo-first” and “pseudo-second” order models are macroscopic kinetic models commonly used for describing adsorption process, which suggest that the adsorption process can be considered as the “first” or “second” order chemical reaction process when the adsorption is rate-controlled step and the resistance of intraparticle diffusion can be neglected [29]. As for intraparticle diffusion model, it is used to describe the adsorption process where the intraparticle diffusion resistance is the rate-controlled step [31].

As summarized in Table 1, the correlation coefficient R^2 for the pseudo-second-order adsorption model has an extremely high value (>0.994), as is also illustrated in Fig. 5(b), and the adsorption capacities calculated by the model are close to those determined by experiments. However, the correlation coefficients R^2 for the pseudo-first-order and the intraparticle diffusion adsorption models are not satisfactory. So it can be concluded that the pseudo-second-order adsorption model can be used to satisfactorily describe the adsorption kinetics of UO_2^{2+} on CTR. Looking at the behavior over the whole adsorption process, it is likely to agree with the suggestion that the chelating interaction of UO_2^{2+} with

Table 1
Adsorption kinetics parameters fitted by the pseudo-first-order rate model, pseudo-second-order rate model and the intraparticle diffusion (initial conc. of UO_2^{2+} = 1.0 mmol/L, pH = 5.0).

T (K)	Pseudo-first-order rate model					Pseudo-second-order rate model				Intraparticle diffusion	
	k_1	$q_{e\,cal}$	$q_{e\,exp}$	Error	R^2	k_2	$q_{e\,cal}$	Error	R^2	k_3	R^2
303	0.022	0.757	0.821	7.795	0.891	0.042	0.828	−0.853	0.994	0.043	0.628
313	0.033	0.865	0.913	5.257	0.948	0.056	0.934	−2.300	0.995	0.051	0.384
323	0.040	0.898	0.952	5.672	0.936	0.063	0.968	−1.680	0.999	0.053	0.320

Error = $(q_{e\,exp} - q_{e\,cal})/q_{e\,exp} \times 10^2$, R^2: correlation coefficient.

Table 2
Comparison of adsorption capacity of CTR and other adsorbents for UO_2^{2+}.

Adsorbent	Adsorption conditions			Adsorption capacity (mmol/g)	Reference
	C_i (mmol/g)	T (K)	pH		
CTR	2.500	303	5.0	1.300	This work
Biomass-PUG	0.42	295	4.7	0.251	[34]
Calcium alginate beads	3.361	298	4.0	1.680	[35]
Starfish and *Pseudomonas putida*	0.004	298	6.0	0.001	[36]
Cyanobacterium water-bloom	2.521	298	7.0	1.033	[37]
Chitin of *Rhizopus arrhizus*	0.420	295	4.0	0.04	[38]
Saccharomyces cerevisiae	4.201	296	4-5	0.660	[39]

C_i: initial concentration of UO_2^{2+} (mmol/L).

CTR should be the rate controlling step [32], and the inner-diffusion resistance of mass transfer can be neglected.

3.2.3. Adsorption isotherms

Fig. 6 presents the adsorption isotherms of UO_2^{2+} on CTR. The adsorption capacity is about 1.3 mmol/g when the equilibrium concentration of UO_2^{2+} is 1.2 mmol/L at 303 K. Table 2 shows the comparison of adsorption capacity of CTR and other adsorbents for UO_2^{2+}, it can be seen that CTR has a relative higher adsorption capacity of UO_2^{2+} than those of other adsorbents. In addition, the adsorption capacity is increased with the increase of temperature, indicating that the adsorption process is an endothermic process in nature [33].

Adsorption isothermal data are further analyzed by the Langmuir and Freundlich models. In general, there is no theoretical model to describe the adsorption isotherms of liquid/solid adsorption. The adsorption isothermal models used in gas/solid adsorption are always used to describe the liquid/solid adsorption. Langmuir model is often used for monolayer adsorption occurred on a homogeneous surface with identical adsorption sites, which can be expressed by the following equation [40]:

$$q_e = \frac{q_m b C_e}{1 + bC_e} \tag{4}$$

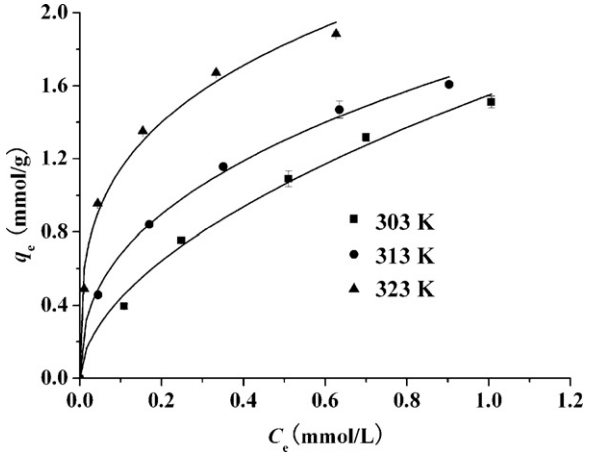

Fig. 6. Adsorption isotherms of CTR to UO_2^{2+}.

where q_e is the amount of UO_2^{2+} adsorbed (mmol/g), C_e is the equilibrium concentration of UO_2^{2+} (mmol/L), and q_m and b are Langmuir constants related to maximum adsorption capacity (monolayer capacity) (mmol/g) and energy of adsorption (L/mmol), respectively. The empirical Freundlich model is appropriate for the adsorption occurred on a heterogeneous surface, which can be expressed by the following equation [41]:

$$q_e = kC_e^{1/n} \tag{5}$$

where q_e and C_e are the same as shown in Eq. (3), k and n are the Freundlich constants related to adsorption capacity and adsorption intensity, respectively.

Table 3 lists the Langmuir and Freundlich parameters and the correlation coefficients (R^2). The adsorption isothermal data are well fitted by the Freundlich equation with correlation coefficients higher than 0.99. In addition, the values of $1/n$ are smaller than 1, indicating that the adsorption process can proceed easily [42].

3.3. Column studies

3.3.1. Effect of bed height

Adsorption columns with different bed depths (7.0, 13.0 and 18.0 cm) are used to investigate the effect of bed height on the adsorption of UO_2^{2+}. UO_2^{2+} solution with concentration of 1.0 mmol/L is pumped into the column at the feeding rate of 0.4 mL/min. The breakthrough curves of column adsorption are presented in Fig. 7(I, II, III). It can be seen that the breakthrough points of these columns are about 54 bed volume (BV), 75 BV, 103 BV, respectively, which indicates that the processing capacity of column is increased as increasing bed height.

Table 3
The Freundlich and Langmuir model parameters of the adsorption of UO_2^{2+} on CTR at pH 5.0.

Temperature (K)	Langmuir constants			Freundlich constants		
	q_m	b	R^2	k	$1/n$	R^2
303	1.907	1.901	0.973	1.513	0.565	0.991
313	1.929	4.892	0.943	1.669	0.397	0.997
323	2.290	22.874	0.984	2.231	0.291	0.990

R^2: correlation coefficient.

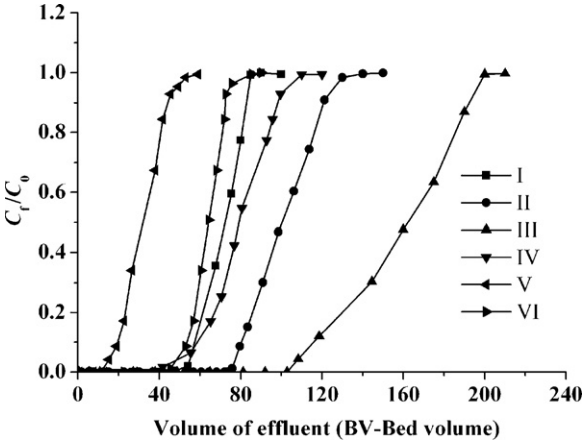

Fig. 7. Breakthrough curves of UO_2^{2+} on CTR (column conditions—I: bed depth = 7.0 cm, feeding rate = 0.4 mL/min, initial conc. of UO_2^{2+} = 0.5 mmol/L; II: bed depth = 13.0 cm, feeding rate = 0.4 mL/min, initial conc. of UO_2^{2+} = 0.5 mmol/L; III: bed depth = 18.0 cm, feeding rate = 0.4 mL/min, initial conc. of UO_2^{2+} = 0.5 mmol/L; IV: bed depth = 7.0 cm, feeding rate = 0.4 mL/min, initial conc. of UO_2^{2+} = 1.0 mmol/L; V: bed depth = 7.0 cm, feeding rate = 0.4 mL/min, initial conc. of UO_2^{2+} = 2.0 mmol/L; VI: bed depth = 13.0 cm, feeding rate = 0.4 mL/min, initial conc. of UO_2^{2+} = 0.5 mmol/L).

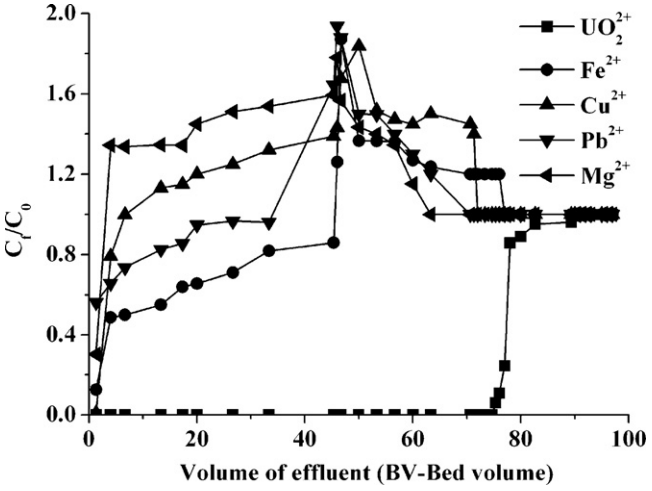

Fig. 8. Effect of co-existing metal ions on the adsorption of UO_2^{2+}.

The slope of breakthrough curves greatly indicates the availability of columns which related with the bed depths. In the adsorption process, the adsorption zone (also called mass transfer zone, where the bulk of adsorption takes place) moves forward as time passes and then approaches the exit of the bed. When the adsorption zone is completely moved out through the column, the concentration of the adsorbate at the exit should equal to the concentration in feeding. The slope of breakthrough curves represents the dimension of adsorption zone. In general, the higher slope of breakthrough curve indicates higher availability of column. In addition, the adsorption capacities of the three columns at breakthrough points are 0.473, 0.379, 0.258 mmol/g, respectively. Therefore, the availability of column is decreased as the increase of the bed depth.

3.3.2. *Effect of initial concentration*

The effect of initial concentrations of UO_2^{2+} on column adsorption is investigated with different initial UO_2^{2+} concentrations viz. 0.5, 1.0 and 2.0 mmol/L. As shown in Fig. 7(I, IV, V), it can be observed that the breakthrough points are 70, 40 and 12 BV with the increase of initial concentration from 0.5 to 2.0 mmol/L. It is found that the adsorption capacities at breakthrough points are 0.379, 0.416 and 0.378 mmol/g, respectively, meaning that the initial concentrations should be in a suitable range for the higher column availability.

3.3.3. *Effect of feeding rate*

Fig. 7(II, VI) shows the breakthrough curves of column adsorption with two different feeding rates. It is found that the breakthrough point are 75 and 44 BV with the increase of feeding rate from 0.4 to 1.0 mL/min, and the adsorption capacity at breakthrough points are 0.379 and 0.228 mmol/g.

At lower feeding rate, the residence time of UO_2^{2+} in column is longer than that of at higher feeding rate. Therefore, the amount of UO_2^{2+} adsorbed on column should be increased. However, the dimension of adsorption zone is increased at lower feeding rate. The ratio of the breakthrough volume to the saturation volume in the column adsorption is an important factor which indicated the efficiency of adsorbent. The saturation volume is defined as the volume when the concentration of UO_2^{2+} in effluent equal to that of feeding solution. It has been reported that 0.5 or larger ratio of breakthrough volume to saturation volume is considered satisfactory for column adsorption [43]. From above column adsorption investigation, it can be concluded that the depth of column, initial concentration of feeding and flow rate should be systemically designed for practical application.

3.3.4. *Effect of co-existing metal ions*

The breakthrough curves of column adsorption of UO_2^{2+} with co-existing metal ions are shown in Fig. 8. To our delight, the presence of co-existing metal ions has almost no effect on the adsorption capacity of CTR to UO_2^{2+}, and the breakthrough point is only slightly in advance, as compared with Fig. 7. The adsorption capacities of Cu^{2+}, Mg^{2+}, Pb^{2+} and Fe^{2+} on CTR are very limited. Interestingly, the shape of breakthrough curves of co-existing metal ions are extraordinary different with that of UO_2^{2+}. The concentration of Cu^{2+}, Mg^{2+}, Pb^{2+} and Fe^{2+} in effluent is even higher than that of feeding solution as the adsorption process proceeded. Compared with Al^{3+}, Cu^{2+} and Fe^{2+}, UO_2^{2+} has much more empty d-orbits, which should favor the donation of electrons from –OH of tannins to UO_2^{2+} [44]. According to the literature [45], the chelating constant of UO_2^{2+} with the adjacent phenolic groups is as high as 15.9. At the early stage of the adsorption process, CTR adsorbent has enough adsorption sites for the adsorption of UO_2^{2+} and co-existing metal ions. Therefore, only low concentration of co-existing metal ions were detected in the effluent of 1–2 BV, as shown in Fig. 8. With the adsorption process processed, the available adsorption sites gradually decreased, which leads to the adsorption sites are inadequate for the adsorption of all metal ions. Due to this reason, UO_2^{2+} with stronger chelating ability began to replace the co-existing metal ions (Cu^{2+}, Mg^{2+}, Pb^{2+} and Fe^{2+}) adsorbed on CTR, and the replaced co-existing metal ions were released into the effluent again. As a result, the co-existing metal ions in the effluent of 3–77 BV exhibited a higher concentration than inlet solution. Other reported biomass adsorbent also exhibited much higher adsorption affinity to UO_2^{2+} when UO_2^{2+} coexists with other metal ions [9]. Above results suggests that CTR has excellent adsorption selectivity to UO_2^{2+}.

Saturated CTR column is regenerated with 0.1 mol/L HNO_3 solution. The typical elution pattern is presented in Fig. 9. It is found that the elution process is very fast, and about 99% of the UO_2^{2+} adsorbed on the column can be recovered using about 6 BV of HNO_3 solution. The maximum UO_2^{2+} concentration in eluent is about 50 mmol/L, that is about 100 times higher than that of inlet solution, while the concentration of the co-existing metal ions in eluent is far below than that of UO_2^{2+}. In addition, the regenerated column is reused. The performance of adsorption-desorption processes is repeated 6 times, and the adsorption capacity and selectivity to

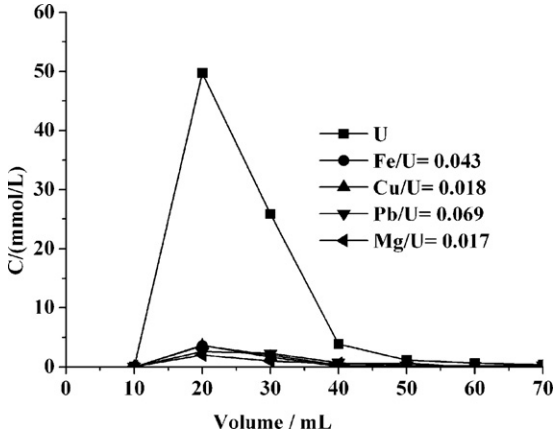

Fig. 9. Desorption curves of CTR column.

UO_2^{2+} are almost un-reduced. Therefore, the CTR are very promising to be used as an effective adsorbent for the recovery of UO_2^{2+} from wastewater.

4. Conclusions

Collagen–tannin resin (CTR) was prepared via reaction of hydrolyzed collagen with black wattle tannin using aldehyde as cross-linking agent. During the preparation process, hydrolyzed collagen was re-assembled into fiber due to the inducement of black wattle tannin. Compared with collagen fiber immobilized tannin (CF-T), the loading amount of tannin on CTR significantly increased, and therefore, the adsorption capacity to UO_2^{2+} considerably increased. Furthermore, CTR exhibited fast adsorption rate, excellent adsorption selectivity and reusability to UO_2^{2+}. Consequently, CTR is a promising adsorbent for the recovery of UO_2^{2+} from practical wastewater.

Acknowledgments

This research was financially supported by The Research Found for the National Natural Science Foundation of China (20976111, 20776090), the National Technologies R&D Program (2006BAC02A09) and Sichuan Province Technologies R&D Program (2008GZ0026).

Appendix A. Supplementary data

Supplementary data associated with this article can be found, in the online version, at doi:10.1016/j.jhazmat.2010.03.002.

References

[1] J.L. Lapka, A. Paulenova, M.Y. Alyapyshev, V.A. Babain, R.S. Herbst, J.D. Law, Extraction of uranium(VI) with diamides of dipicolinic acid from nitric acid solutions, Radiochim. Acta 97 (2009) 291–296.
[2] C. Riordan, M. Bustard, R. Putt, A.P. McHale, Removal of uranium from solution using residual brewery yeast: combined biosorption and precipitation, Biotechnol. Lett. 19 (1997) 385–387.
[3] R. Ganesh, K.G. Robinson, L.L. Chu, D. Kucsmas, G.D. Reed, Reductive precipitation of uranium by desulfovibrio desulfuricans: evaluation of cocontaminant effects and selective removal, Water Res. 33 (1999) 3447–3458.
[4] K. Vaaramaa, S. Pulli, J. Lehto, Effects of pH and uranium concentration on the removal of uranium from drinking water by ion exchange, Radiochim. Acta 88 (2000) 845–849.
[5] S.B. Xie, C. Zhang, X.H. Zhou, J. Yang, X.J. Zhang, J.S. Wang, Removal of uranium(VI) from aqueous solution by adsorption of hematite, J. Environ. Radioactiv. 100 (2009) 162–166.
[6] A. Gajowiak, M. Majdan, K. Drozdzal, Sorption of uranium(VI) on clays and clay minerals, Przem. Chem. 88 (2009) 190–196.
[7] Zhuravlev, O. Zakutevsky, T. Psareva, V. Kanibolotsky, V. Strelko, M. Taffet, G. Gallios, Uranium sorption on amorphous titanium and zirconium phosphates modified by Al^{3+} or Fe^{3+} ions, J. Radioanal. Nucl. Chem. 254 (2002) 85–89.
[8] K. Oshita, M. Oshima, Y.H. Gao, K.H. Lee, S. Motomizu, Synthesis of novel chitosan resin derivatized with serine moiety for the column collection/concentration of uranium and the determination of uranium by ICP-MS, Anal. Chim. Acta 480 (2003) 239–249.
[9] J. Choi, J.W. Park, Competitive adsorption of heavy metals and uranium on soil constituents and microorganism, Geosci. J. 9 (2005) 53–61.
[10] T.S. Anirudhan, P.S. Suchithra, Synthesis and characterization of tannin-immobilized hydrotalcite as a potential adsorbent of heavy metal ions in effluent treatments, Appl. Clay. Sci. 42 (2008) 214–223.
[11] A. Nakajima, T. Sakaguchi, Recovery of uranium by tannin immobilized on agarose, J. Chem. Technol. Biotechnol. 40 (1987) 223–232.
[12] T. Sakaguchi, A. Nakajima, Recovery of uranium from seawater by immobilized tannins, Sep. Sci. Technol. 22 (1987) 1609–1623.
[13] Chibata, T. Tosa, T. Mori, Z. Watanabe, N. Sakata, Immobilized tannin—a novel adsorbent for protein and metal ion, Enzyme Microb. Technol. 8 (1986) 130–136.
[14] A. Nakajima, T. Sakaguchi, Recovery of uranium by tannin immobilized on matrices which have amino group, J. Chem. Technol. Biotechnol. 47 (1990) 31–38.
[15] Z.B. Lu, X.P. Liao, B. Shi, The reaction of vegetable tannin–aldehyde–collagen: a further understanding of vegetable tannin–aldehyde combination tannage, J. Soc. Leath. Technol. Chem. 87 (2004) 173–178.
[16] X.P. Liao, Z.B. Lu, X. Du, X. Liu, B. Shi, Collagen fiber immobilized myrica rubra tannin and its adsorption to UO_2^{2+}, Environ. Sci. Technol. 38 (2004) 324–328.
[17] R. Wang, X.P. Liao, S.L. Zhao, B. Shi, Adsorption of bismuth(III) by bayberry tannin immobilized on collagen fiber, J. Chem. Technol. Biotechnol. 81 (2006) 1301–1306.
[18] X.Y. Lu, A brief discussion on manufacture of hide powder for tannin analysis, Linchan Huaxue Yu Gongye 20 (2000) 71–74 (in Chinese).
[19] W. Friess, Collagen-biomaterial for drug delivery, Eur. J. Pharm. Biopharm. 45 (1998) 113–136.
[20] M.C. Goh, M.F. Paige, M.A. Gale, I. Yadegari, M. Edirisinghe, J. Strzelczyk, Fibril formation in collagen, Phys. A 239 (1997) 95–102.
[21] J.R. Harris, A. Reiber, H.A. Therese, W. Tremel, Molybdenum blue: binding to collagen fibres and microcrystal formation, Micron 36 (2005) 387–391.
[22] C. Guo, L.J. Kaufman, Flow and magnetic field induced collagen alignment, Biomaterials 28 (2007) 1105–1114.
[23] Z.B. Lu, X.P. Liao, D.H. Sun, Reaction of vegetable tannin–aldehyde–collagen—a further understanding on vegetable tannin–aldehyde combination tannage, Linchan Huaxue Yu Gongye 24 (2004) 7–11 (in Chinese).
[24] L.S. Balistrieri, J.W. Murray, The surface chemistry of goethite (alpha FeOOH) in major ion seawater, Am. J. Sci. 281 (1981) 788–806.
[25] S.M. Yu, C.L. Chen, P.P. Chang, T.T. Wang, S.S. Lu, X.K. Wang, Adsorption of Th(IV) onto Al-pillared rectorite: effect of pH, ionic strength, temperature, soil humic acid and fulvic acid, Appl. Clay. Sci. 38 (2008) 219–226.
[26] M.J. Charrier, I. Saucedo, E. Guibal, P. Le Cloirec, Approach of uranium sorption mechanisms on chitosan and glutamate glucan by IR and ^{13}C NMR analysis, React. Funct. Polym. 27 (1995) 209–221.
[27] S. Lagergreen, About the theory of so called adsorption of soluble substances, Kung. Sven. Veten. Hand. 24 (1898) 1–39.
[28] Y.S. Ho, Citation review of Lagergreen kinetic rate equation on adsorption reaction, Scientometrics 59 (2004) 171–177.
[29] Y.S. Ho, G. McKay, Pseudo-second order model for sorption processes, Process Biochem. 34 (1999) 451–465.
[30] M.S. Chiou, H.Y. Li, Adsorption behavior of reactive dye in aqueous solution on chemical cross-linked chitosan beads, Chemosphere 50 (2003) 1095–1105.
[31] V. Vadivelan, K.V. Kumar, Equilibrium, kinetics, mechanism, and process design for the sorption of methylene blue onto rice husk, J. Colloid Interface Sci. 286 (2005) 90–100.
[32] P. Fornasiero, J. Kašpar, M. Graziani, On the rate determining step in the reduction of CeO_2–ZrO_2 mixed oxides, Appl. Catal. B Environ. 22 (1999) 11–14.
[33] Y. Bulut, H. Aydin, A kinetics and thermodynamics study of methylene blue adsorption on wheat shells, Desalination 194 (2006) 259–267.
[34] M.Z.C. Hu, M. Reeves, Biosorption of uranium by *Pseudomonas aeruginosa* strain CSU immobilized in a novel matrix, Biotechnol. Prog. 13 (1997) 60–70.
[35] C. Gok, S. Aytas, Biosorption of uranium(VI) from aqueous solution using calcium alginate beads, J. Hazard. Mater. 168 (2009) 369–375.
[36] J. Choi, J.Y. Lee, J.S. Yang, Biosorption of heavy metals and uranium by starfish and *Pseudomonas putida*, J. Hazard. Mater. 161 (2009) 157–162.
[37] P.F. Li, Z.Y. Mao, X.J. Rao, X.M. Wang, M.Z. Min, L.W. Qiu, Z.L. Liu, Biosorption of uranium by lake-harvested biomass from a cyanobacterium bloom, Bioresour. Technol. 94 (2004) 193–195.
[38] M. Tsezos, The role of chitin in uranium adsorption by *R. arrhizus*, Biotechnol. Bioeng. 25 (2004) 2025–2040.
[39] N. Kuyucak, B. Volesky, Biosorbents for recovery of metals from industrial solutions, Biotechnol. Lett. 10 (1988) 137–142.
[40] Langmuir, The constitution and fundamental properties of solids and liquids, J. Am. Chem. Soc. 38 (1916) 2221–2295.
[41] N.P. Coutrin, S. Altenor, S. Gaspard, Assessment of the surface area occupied by molecules on activated carbon from liquid phase adsorption data from a combination of the BET and the Freundlich theories, J. Colloid Interface Sci. 332 (2009) 515–519.

[42] F. Haghseresht, G.Q. Lu, Adsorption characteristics of phenolic compounds onto coal-reject-derived adsorbents, Energy Fuel 12 (1998) 1100–1107.
[43] A.C.Q. Ladeira, C.A. Morais, Uranium recovery from industrial effluent by ion exchange-column experiments, Miner. Eng. 18 (2005) 1337–1340.
[44] R.T. Gephart, N.J. Williams, J.H. Reibenspies, A.S. De Sousa, R.D. Hancock, Complexation of metal ions of higher charge by the highly preorganized tetradentate ligand 2,9-bis(hydroxymethyl)-1, 10-phenanthroline. A crystallographic and thermodynamic study, Inorg. Chem. 48 (2009) 8201–8209.
[45] W.J. Bair, H.C. Hodge, J.N. Stannard, J.B. Hursh, Uranium–plutonium–transplutonic elements, in: H.C. Hodge, J.N. Stannard, J.B. Hursh (Eds.), Physical and Chemical Properties of Uranium, Springer-Verlag, Berlin, 1973, pp. 197–240.